Am J Transl Res 2020;12(10):6204-6219
www.ajtr.org /ISSN:1943-8141/AJTR0106944

Original Article

Clostridium difficile toxin B-induced colonic inflammation is mediated by the FOXO3/PPM1B pathway in fetal human colon epithelial cells

Qingqing Xu[1,2*], Ying Li[1,2*], Yuejuan Zheng[3], Yijian Chen[1,2], Xiaogang Xu[1,2], Minggui Wang[1,2]

[1]Institute of Antibiotics, Huashan Hospital, Fudan University, Shanghai 200040, China; [2]Key Laboratory of Clinical Pharmacology of Antibiotics, National Health and Family Planning Commision, Shanghai 200040, China; [3]Department of Immunology and Microbiology, Shanghai University of Traditional Chinese Medicine, Shanghai 201203, China. [*]Equal contributors.

Received December 25, 2019; Accepted August 1, 2020; Epub October 15, 2020; Published October 30, 2020

Abstract: *Clostridium difficile* (*C. difficile*) toxin B (TcdB) is as an inflammatory enterotoxin that accounts for manifestations of widespread healthcare-associated *C. difficile* infection, including colonic inflammation. The present work explored the molecular mechanism by which TcdB activates innate immunity and stimulates pro-inflammatory cytokine release. Fetal human colon epithelial cells (FHCs) were treated with recombinant TcdB protein. Cell growth inhibition and apoptosis were measured with Cell Counting Kit-8 and Annexin V-fluorescein isothiocyanate Apoptosis Detection Kit, respectively. Flow cytometry analysis was also performed. Inflammatory cytokine induction was determined with enzykeme-linked immunosorbent assay analyses. Protein expression was assessed by western blot analysis. Gene overexpression and knockdown were performed with lentiviral transduction. Real-time quantitative polymerase chain reaction was used to examine gene expression. Dual-luciferase reporter assays and chromatin immunoprecipitation were implemented to explore transcriptional regulation. Mouse colon tissues were analyzed with hematoxylin and eosin staining. The results show that TcdB-induced cell growth and apoptosis and enhanced expression of interleukin-6 and tumor necrosis factor alpha in FHCs. We identified protein phosphatase magnesium-dependent 1B (PPM1B) as the key mediator promoting the phosphorylation of nuclear factor-κB p65, which accounted for the increase in pro-inflammatory cytokines. The findings demonstrate that PPM1B expression is directly regulated by the AKT/FOXO3 signaling pathway in FHCs. We confirmed the molecular mechanism with *in vivo* studies using a mouse model infected with *C.* difficile and treated with a phosphoinositide 3-kinase/AKT signaling inhibitor. In conclusion, TcdB induces inflammation in human colon epithelial cells by regulating the AKT/FOXO3/PPM1B pathway.

Keywords: Clostridium difficile toxin B (TcdB), human colon epithelial cell, protein phosphatase magnesium-dependent 1B (PPM1B), Forkhead box O3 (FOXO3)

Introduction

Clostridium difficile (*C. difficile*) infection (CDI) is the most common cause of healthcare-associated diarrhea in developed countries [1, 2]. The disease ranges from mild to severe diarrhea or even fatal colonic inflammation. Over the past decade, increased morbidity and lethality from CDI has increased demand for new treatment options [3, 4]. Induced by antibiotic treatment or disruption of the normal gastrointestinal flora, CDI is characterized by an intense inflammatory response including increased inflammatory cytokines such as interleukin-6 (IL-6), tumor necrosis factor alpha (TNF-α), and others [5, 6].

The two large glucosylating toxins, TcdA and TcdB, are primarily responsible for colonic inflammation [7]. Burdon et al. revealed a direct relationship between toxin levels and the development of pseudomembranous colitis and diarrhea duration [8]. However, there has been considerable debate regarding the relative importance of TcdA and TcdB in infection in recent decades [7]. Early experiments with purified toxins suggested that TcdB did not cause any significant response unless it was mixed with

TcdA [9]. In contrast, Lyras et al. reported that TcdB is essential for *C. difficile* virulence, while a strain producing TcdA alone was avirulent [10]. Consistent with this, work by Kuehne and colleagues confirmed the importance of TcdB in virulence [11].

As a homologous glycosyltransferase, TcdB can inhibit a group of small GTPases within host cells [12]. Previous studies revealed that TcdB can exert significant antiproliferative effects *in vitro* [13-15]. To date, numerous studies have reported on the potential mechanism of action of TcdB. Chen et al. reported that TcdB can glucosylate Rho proteins, which inhibits their interaction with effectors and thus blocks Rho-dependent cell signaling, causing cytotoxic effects [16, 17]. Qa et al. found that TcdB can induce both caspase-dependent and caspase-independent apoptotic pathways *via* the involvement of mitochondrial ATP-dependent potassium channels [18]. Additionally, a variety of pathways were proposed to lead to inflammasome activation [19], the response to MyD88-dependent inflammatory signaling [20], and the production of Rac-dependent reactive oxygen species [21]. However, the molecular basis of the mechanism by which TcdB stimulates pro-inflammatory cytokine release [7] remains unclear.

Nuclear factor-κB (NF-κB) plays a central role in the inflammatory response to infection and tissue injury by controlling the activation of a variety of genes such as IL-6 [23]. NF-κB transcriptional activity can be regulated by a collection of protein kinases and phosphatases [24, 25]. Among them, protein phosphatase magnesium-dependent 1A (PPM1A) and PPM1B are required for the regulation of TNF-α-induced NF-κB-dependent IL-6 gene expression [26], while PPM1D directly dephosphorylates NF-κB [24]. In addition, the expression of dual specificity phosphatase (DUSP), a regulator for inflammatory cytokine production [27], inversely correlates with NF-κB activity [28]. Similarly, the transcription factor FOXO3 is controlled by the protein kinase AKT [29], which determines FOXO3 shuttling between the nucleus and cytoplasm and thus regulation of FOXO3 transcriptional activity [29, 30]. To our knowledge, the relationship between NF-κB and TcdB function remains unknown. There are also few reports exploring the potential role of these transcription factors in the context of TcdB-induced intestinal inflammatory disease (*e.g.,* colitis).

In the present study, we investigated the molecular mechanism underlying TcdB-induced colonic inflammation. As a model system, we treated fetal human colon epithelial cells (FHCs) with recombinant TcdB protein. Our experiments identified PPM1B as a key mediator in decreasing the phosphorylation of NF-κB p65 (RelA) and pro-inflammatory cytokine production. Furthermore, we revealed that PPM1B expression was directly regulated by the AKT/FOXO3 signaling in FHCs, which could be the molecular basis underlying TcdB-induced colitis. Moreover, *in vivo* studies with a mouse model infected with *C. difficile* and treated with a phosphoinositide 3-kinase (PI3K)/AKT inhibitor confirmed the mechanism and could be developed as a future treatment.

Materials and methods

Reagents, antibodies, and cell line

Recombinant *C. difficile* toxin B (TcdB) was purchased from R&D Systems (Minneapolis, MN, USA). The protease inhibitor cocktail and phosphatase inhibitor cocktail were purchased from Sigma Aldrich (St Louis, MO, USA). The PI3K/AKT signaling inhibitor LY294002 was purchased from Selleck Chemicals (Houston, TX, USA). The bicinchoninic acid (BCA) Protein Assay Kit, Lipofectamine 2000 Transfection Reagent, TRIzol Reagent, RevertAid First Strand cDNA Synthesis Kit, and Maxima SYBR Green/ROX qPCR Master Mix (2×) were purchased from Thermo Fisher Scientific, Inc. (Waltham, MA, USA). Antibodies against PPM1A, PPM1B, IL-6, TNF-α, AKT, P-AKT (T308), NF-κB p65, P-NF-κB p65 (S536), FOXO3, and P-FOXO3 (S253) were purchased from Abcam (Cambridge, UK). The antibody against glyceraldehyde 3-phosphate dehydrogenase (GAPDH) was purchased from Cell Signaling Technology (Danvers, MA, USA). *C. difficile* strains were provided by Huashan Hospital, Fudan University (Shanghai, China). FHCs were purchased from the Cell Bank at the Shanghai Institutes for Biological Sciences, Chinese Academy of Sciences (Shanghai, China) and cultured in Ham's F12 medium containing 45% Dulbecco's minimum essential medium (DMEM), 25 mM HEPES, 10 ng/mL cholera toxin, 0.005 mg/mL

insulin, 0.005 mg/mL transferrin, 100 ng/mL hydrocortisone, and 10% fetal bovine serum at 37°C.

Animals

Female adult BABL/c mice (20±2 g) were obtained from B&K Universal Group Limited, (Shanghai, China). All experiments were performed according to protocols approved by the Animal Studies Subcommittee of Huashan Hospital, Fudan University. The approval file (file number: 20160911A243) of animal experiments is provided in the Supplementary Materials. BABL/c mice were randomly divided into control, model, and model + LY294002 groups with 12 mice in each. For the control group, 0.5 mL saline was administered once; the model group received 0.5 mL (1×10^8 CFU/mL) C. difficile that was intragastrically administered. The model + LY294002 group also received a daily intraperitoneal injection of LY294002 solution (5 mg/kg). Six mice were sacrificed in each group at 1 and 3 days, and the serum was stored at -80°C. Colon tissues were fixed in 4% paraformaldehyde for subsequent pathological examination, and a subset were frozen at -80°C for subsequent western blot detection.

Vector construction

The PPM1B and FOXO3 overexpression vector was constructed by cloning the cDNAs of human PPM1B and FOXO3 into a pLVX-Puro vector (Clontech, Mountain View, CA, USA) using the EcoRI and BamHI restriction sites. Short hairpin RNAs (shRNAs) designed to target the sequence (CAATGTGTTTCAACTTTAA) of the FOXO3 transcript were cloned into the lentiviral shRNA vector pLKO.1. The forward sequence was 5'-CCGGCAATGTGTTTCAACTTTAACTCGAGTTAAAGTTGAAACACATTGTTTTT-3', and the reverse sequence was 5'-AATTAAAAACAATGTGTTTCAACTTTAACTCGAGTTAAAGTTGAAACACATTG-3'. The pGL3-basic-PPM1B-p plasmid used in the dual-luciferase reporter assay was constructed by inserting the promoter of human PPM1B (NM_002706.5) into the pGL3-basic luciferase reporter vector (Promega, Madison, WI, USA). All of the constructs were confirmed by sequencing.

Gene overexpression and knockdown

FOXO3 was knocked down with a pLKO-based lentiviral vector. pLVX-Puro retroviral vectors were used for the overexpression of PPM1B and FOXO3. Lentiviruses were generated in HEK293T cells as previously described [31], then FHCs were infected with the virus-containing supernatants. Changes in expression of PPM1B and FOXO3 were confirmed by quantitative real-time PCR (qPCR) and western blotting analysis (Supplementary Figure 1).

Cell proliferation assay

Cell proliferation was monitored using a Cell Counting Kit-8 (CCK-8, SAB Biotech, College Park, MD, USA) according to the manufacturer's instructions. FHCs subjected to different treatments were seeded into 96-well plates (3×10^3 cells/well). At different time points (*e.g.,* 0, 24, 48, and 72 h), the medium in each well was changed to 100 µl containing CCK-8 (the volume ratio of DMEM:CCK-8 was 9:1). After incubation at 37°C for 1 h, the number of viable cells was assessed by measuring absorbance at 450 nm using a microplate reader.

Apoptosis assay

Apoptotic cells were assessed by staining with Annexin V and propidium iodide (PI) using an Annexin V- fluorescein isothiocyanate (FITC) Apoptosis Detection Kit (Beyotime Institute of Biotechnology, Shanghai, China) following the instructions in the manual. Briefly, 1×10^6 FHCs were collected, washed, and resuspended in 195 µL Annexin V-FITC binding buffer. After that, the cells were incubated with Annexin V-FITC (5 µL) and PI (5 µL) in the dark for 15 min. Then, apoptosis was detected using an Accuri C6 flow cytometer (BD Biosciences, Franklin Lakes, NJ, USA).

Enzyme-linked immunosorbent assay (ELISA)

Cell culture supernatants or peripheral blood were collected at different time points. Concentrations of cytokines (IL-6 and TNF-α) were analyzed using human IL-6 and TNF-α ELISA kits, as well as mouse IL-6 and TNF-α ELISA kits from JRDUN Biotechnology Co., Ltd. (Shanghai, China) following the manufacturer's instructions. For each well, absorbance at 450 nm was measured with a microplate reader. The concentrations of IL-6 and TNF-α in samples were determined by comparing the optical density to the standard curve.

Western blot analysis

The collected FHCs or intestinal tissues were lysed in radioimmunoprecipitation assay buffer containing a protease inhibitor cocktail and a phosphatase inhibitor cocktail on ice. After centrifugation, the supernatants were collected, and the protein concentration was quantified with BCA reagents. Protein lysates (25 or 50 μg per lane for each individual cell/tissue sample) were subjected to 10% sodium dodecyl sulfate-polyacrylamide gel electrophoresis. The samples were transferred to polyvinylidene fluoride membranes using a semidry protein transfer system, blocked (5% milk) and incubated with primary antibodies against PPM1A, PPM1B, IL-6, TNF-α, AKT, P-AKT (T308), NF-κB p65, P-NF-κB p65 (S536), FOXO3, P-FOXO3 (S253), and GAPDH. After washing, they were further incubated with an appropriate horseradish peroxidase-conjugated secondary antibody. Finally, the samples were detected with an enhanced chemiluminescence system.

Dual-luciferase reporter assay

pGL3-basic-PPM1B-p (1.5 μg) was transfected into FHCs together with 20 ng pRL Renilla luciferase control reporter vector (Promega) using the Lipofectamine 2000 reagent. After 48 h, the luciferase and Renilla luciferase activities were measured with the dual-luciferase assay system (Promega). Then, the signals of firefly luciferase activity were normalized to that of the Renilla luciferase activity.

Chromatin immunoprecipitation (ChIP)

ChIP experiments were performed as previously reported [32]. Briefly, FHCs in the log-phase were fixed with 1% formaldehyde at room temperature for 10 min, which was then stopped by the addition of glycine to a final concentration of 0.125 M. Cells were collected for nuclei isolation. The prepared samples were digested and sonicated. After centrifugation, the solution was collected and incubated with rabbit anti-FOXO3 or rabbit polyclonal antibody at 4°C overnight. Immunoprecipitation, washing, and elution of the immune complexes were carried out sequentially. Afterwards, the cross-links were reversed, and the RNA and protein were removed by RNAse and proteinase K, respectively. Finally, qPCR was used to amplify the eluted DNA with specific primers for the PPM1B promoter (forward: 5'-ACTGACCCGCAAGAAAGC-3', reverse: 5'-CAAACACCGCCCACTAAG-3').

RNA isolation and real-time qPCR

Total RNA was extracted from the cultured cells with the TRIzol reagent according to the standard manual. RNA was reverse transcribed using the RevertAid First Strand cDNA Synthesis Kit before quantification with spectrophotometry. Maxima SYBR Green/ROX qPCR Master Mix was used for real-time qPCR experiments. GAPDH was used as an internal control. The specific primers used in real-time qPCR are shown in **Table 1**.

Animal experiments

Mice were randomly divided into three groups. Mice in the blank group received a single intragastric administration of saline (0.5 mL) on day 0 as a control. Mice in the model group were intragastrically administered *C. difficile* (1×10^8 CFU/mouse) on day 0. After intragastric administration of *C. difficile* (1×10^8 CFU/mouse) on day 0, mice in the drug treatment group received a daily intraperitoneal injection of LY294002 (5 mg/kg). Six mice/group were euthanized on days 1 and 3. Blood and colon tissue samples were collected for further examination. The concentrations of IL-6 and TNF-α in the mouse serum were determined using mouse IL-6 and TNF-α ELISA kits according to the standard manuals.

Hematoxylin & eosin (H&E) staining

The resected colon tissues were fixed in 4% formaldehyde buffered with phosphate-buffered saline and then embedded in paraffin. The 6-μm-thick sections were stained with H&E for histological analysis according to a previously described method [33].

Statistical analysis

All experiments were performed in triplicate, and the results are expressed as mean ± SD. One-way analysis of variance followed by least significant difference post hoc tests were used to compare differences between groups. Data were analyzed using SPSS 15 software (Chicago, IL, USA). Differences were considered statistically significant at $P<0.05$.

Table 1. Real-time PCR primer sequences

Gene	Accession number	Primer sequence	Fragment length
DUSP1	NM_004417.3	fwd: AGTACCCCACTCTACGATCAGG	77 bps
		rev: GAAGCGTGATACGCACTGC	
DUSP2	NM_004418.3	fwd: TAGACGCTATACCGTGGACTC	215 bps
		rev: GTGAAAGGCTCACAGACAGAC	
PPM1A	NM_021003.4	fwd: TAACTGTGGAGACTCAAGAGGTT	216 bps
		rev: AGCTGCTCAGTAGGACCTTTT	
PPM1B	NM_001033557.2	fwd: TGGGAATGGTTTACGTTATGGC	94 bps
		rev: GCCGTGAGGAATACCTACAACAG	
PPM1D	NM_003620.3	fwd: CTGTACTCGCTGGGAGTGAG	88 bps
		rev: GTTCGGGCTCCACAACGATT	
FOXO3	NM_001455.3	fwd: CGGACAAACGGCTCACTCT	150 bps
		rev: GGACCCGCATGAATCGACTAT	
GAPDH	NM_001256799.1	fwd: CACCCACTCCTCCACCTTTG	110 bps
		rev: CCACCACCCTGTTGCTGTAG	

Results

TcdB treatment inhibited cell growth and induced apoptosis in FHCs

It is known that TcdB induces intestinal injury and inflammation by disrupting the intestinal epithelial barrier and inducing pro-inflammatory mediators [34]. To gain insight into the potential mechanism, we treated FHCs with recombinant TcdB at different concentrations (600 and 1,000 ng/mL), that were selected based on cellular studies in previous reports [35-37]. We also determined the full titration of TcdB in different concentrations ranging from 100 to 4,800 ng/mL (data not shown). Because intestinal injury primarily influences cell proliferation and survival, we first evaluated the conditions of FHC growth using CCK-8 assays. TcdB significantly inhibited cell growth after 24 h at both doses ($P<0.05$ and $P<0.01$) (**Figure 1A**). The inhibition was much stronger after 48 h ($P<0.001$), and exhibited a time-dependent response (to 72 h). Moreover, we observed that TcdB treatment resulted in marked apoptosis at both concentrations ($P<0.001$) in FHCs (**Figure 1B**). Taken together, our results suggested that TcdB can exert cytotoxic and apoptosis-inducing effects in FHCs, which is in agreement with previous research [38].

TcdB treatment stimulated IL-6 and TNF-α expression and secretion

Previous studies revealed that TcdB can cause inflammation when entering colonic epithelial cells [38]. On this basis, we assessed the induction of the pro-inflammatory cytokines IL-6 and TNF-α by TcdB in FHCs using western blotting and ELISAs. As expected, western blot analysis showed markedly increased expression of IL-6 and TNF-α in TcdB-treated FHCs (**Figure 1C** and Supplementary Figure 2). Moreover, the ELISA data indicated that the TcdB treatment at both concentrations significantly promoted the secretion of both cytokines as early as 12 h ($P<0.001$) (**Figure 1D** and **1E**). The inductions followed a time-dependent pattern in the 48 h following treatment, with statistical significance ($P<0.001$).

TcdB treatment enhanced the phosphorylation of NF-κB p65 (RelA)

The NF-κB family of transcription factors, which consists of five different members, plays critical roles in controlling inflammation, the immune response, and anti-apoptotic responses [39-41]. Among them, NF-κB p65, a subunit of the NF-κB transcription complex, plays an essential role in constitutive IL-6 production and inflammation [41]. We focused on the crucial NF-κB p65 member, which can be affected by numerous signaling molecules. Both doses of TcdB significantly enhanced the phosphorylation of NF-κB p65 at S536 (600 ng/mL: $P<0.05$, 1,000 ng/mL: $P<0.001$) (**Figure 2A**, **2B** and Supplementary Figure 3), which represents an activating phosphorylation marker for canonical NF-κB activation [42]. In contrast, TcdB did not significantly change the total amount of protein, suggesting that the treatment with TcdB only stimulated the transcriptional activity of NF-κB.

TcdB treatment strongly decreased PPM1B expression

The phosphorylation level of NF-κB p65 can be regulated by some phosphatases including PPM1A, PPM1B, and PPM1D [24, 26]. The expression of DUSP, the regulator for inflammatory cytokine production [27], inversely corre-

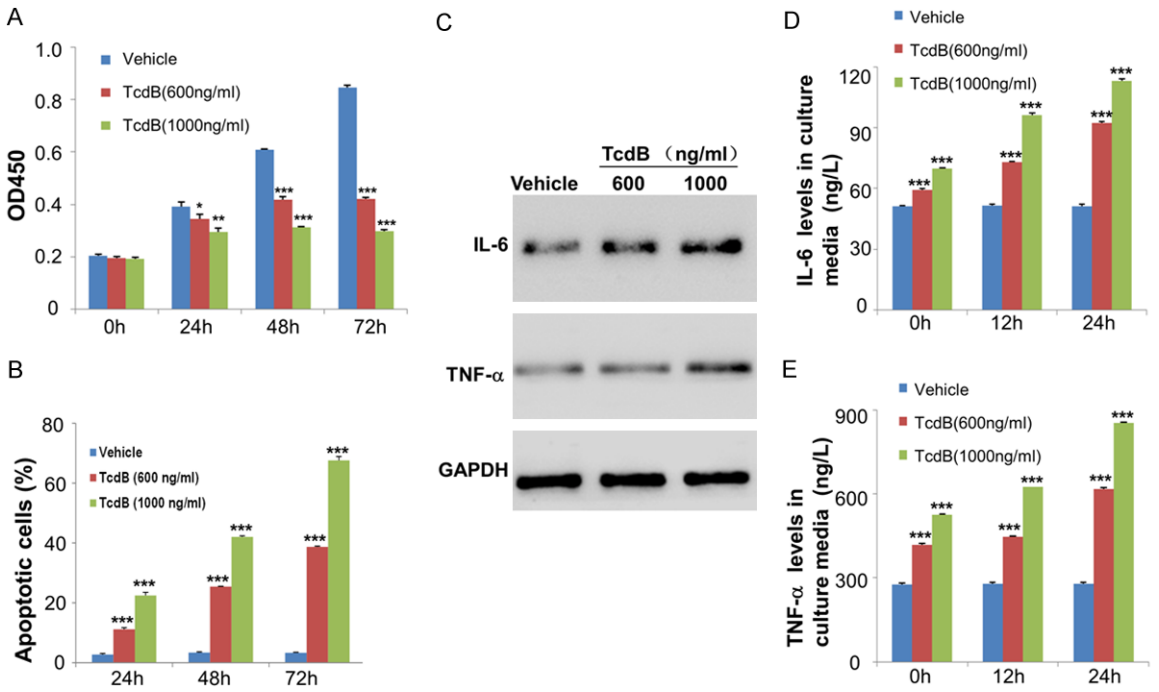

Figure 1. TcdB treatment inhibited cell growth, induced apoptosis, and increased the expression and secretion of IL-6 and TNF-α in FHCs. FHCs were treated with TcdB (600 or 1,000 ng/mL) or Vehicle. A. CCK-8 assays were performed to assess cell growth. B. Annexin V-FITC staining followed by flow cytometry analysis was conducted to evaluated apoptosis. C. Changes in IL-6 and TNF-α expression were measured in FHCs treated with TcdB for 24 h using western blotting analysis. D and E. Changes in IL-6 and TNF-α release were determined by ELISA. Asterisks indicate significant differences (*P<0.05, ***P<0.001) between TcdB-treated and vehicle control cells. Independent experiments were repeated performed to calculate mean values.

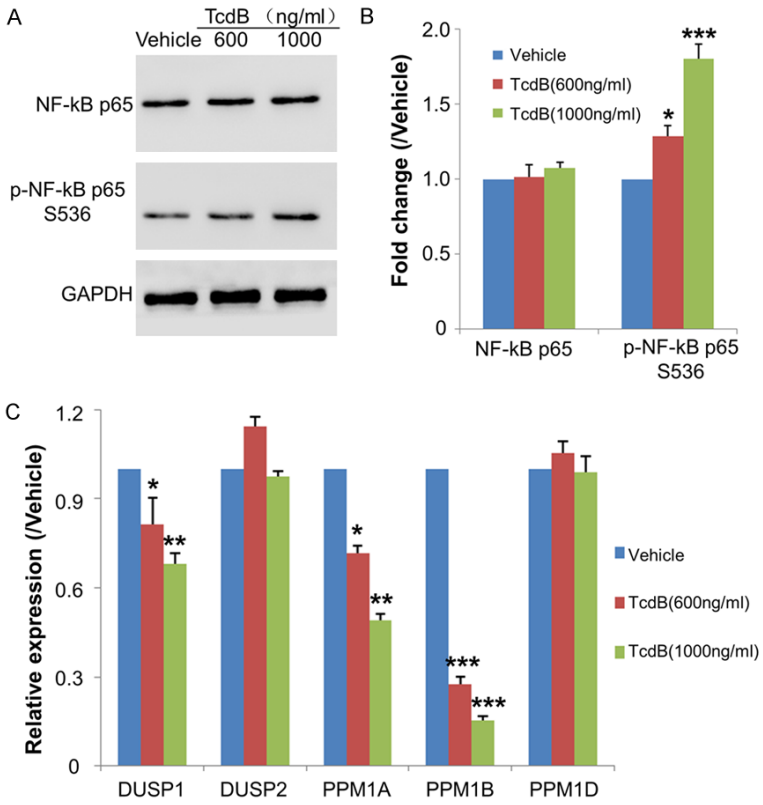

Figure 2. TcdB treatment enhanced the phosphorylation of NF-κB p65 (RelA) and strongly decreased PPM1B expression. A. FHCs were treated with TcdB (600 or 1,000 ng/mL) for 3 h, and the expression and phosphorylation of NF-κB p65 at S536 were examined by western blotting. B. Quantitative results of the western blotting analysis in A. C. FHCs were treated with TcdB (600 or 1,000 ng/mL), and the mRNA expression of selected phosphatases in FHCs were examined by real-time PCR. Asterisks indicate significant differences (*P<0.05, **P<0.01, ***P<0.001) between TcdB-treated and vehicle control cells. Independent experiments were repeated performed to calculate mean values.

lates with NF-κB activity [28]. We investigated the effects of TcdB on these phosphatases with real-time qPCR. We observed that 600 ng/mL TcdB

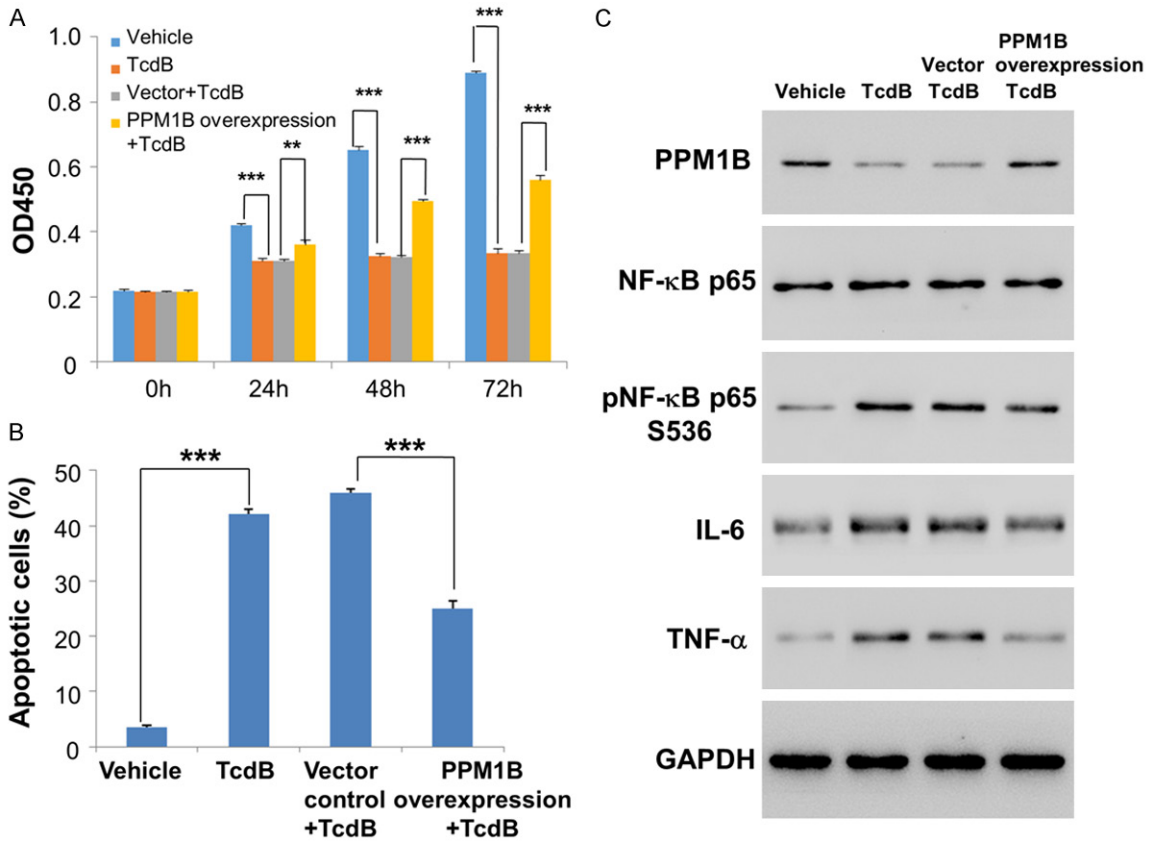

Figure 3. Effects of PPM1B overexpression on cell growth, apoptosis induction, and expression and phosphorylation of selected proteins. FHCs with or without PPM1B overexpression were incubated in the presence or absence of 1,000 ng/mL TcdB. A. CCK-8 assays were performed to assess cell growth. B. Annexin V-FITC staining followed by flow cytometry analysis was conducted to evaluated apoptosis. C. Expression and phosphorylation of selected proteins were assessed with western blotting analysis. Asterisks indicate significant differences (**P<0.01, ***P<0.001). Independent experiments were repeated performed to calculate mean values.

significantly decreased the expression of PPM1A (P<0.05), PPM1B (P<0.001) and DUSP1 (P<0.05) in FHCs (**Figure 2C**). The downregulation of PPM1B, which decreased by >70% (600 ng/mL) and 80% (1,000 ng/mL), was the most significant among these phosphatases. This result prompted us to hypothesize that PPM1B may mediate the induction of inflammation by TcdB in FHCs.

PPM1B overexpression partly blocked the cytotoxic and inflammatory effects of TcdB

To study the role of PPM1B in the context of TcdB-induced colonic inflammation, we overexpressed PPM1B in FHCs and assessed its counteracting effects against TcdB. Compared with TcdB alone, PPM1B overexpression significantly alleviated the cell growth inhibition caused by TcdB from 24 h (P<0.01) to 72 h (P<0.001) (**Figure 3A**). Consistently, PPM1B overexpression also reduced TcdB-induced apoptosis in FHCs (P<0.001) (**Figure 3B**), implying a potential role of PPM1B in mediating the cytotoxic effects of TcdB on FHCs.

We also evaluated the effects on protein expression and phosphorylation. PPM1B overexpression decreased the expression of IL-6 and TNF-α in TcdB-treated FHCs to levels comparable to the vehicle controls (**Figure 3C** and Supplementary Figure 4). PPM1B overexpression also downregulated the phosphorylation of NF-κB p65 at S536 without affecting the total amount of protein. Taken together, these results indicated that PPM1B overexpression could at least partially block the cytotoxic and inflammation-inducing effects of TcdB in FHCs.

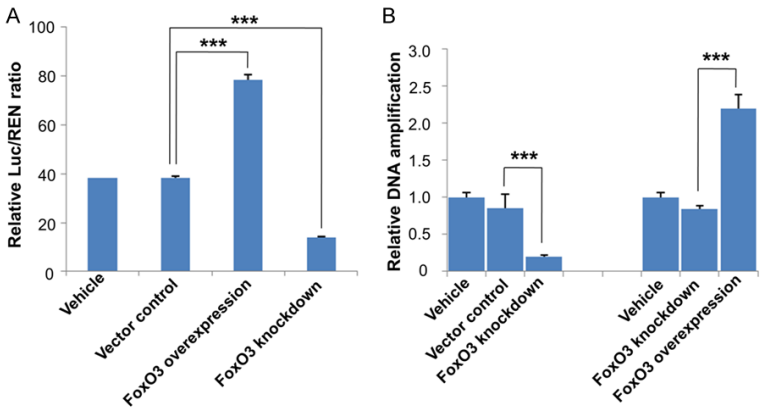

Figure 4. FoxO3 directly regulated PPM1B transcription in FHCs. A. FHCs with either knockdown or overexpression of FOXO3 were subjected to dual-luciferase reporter assays. The activities of firefly luciferase (LUC) and Renilla luciferase (REN) were measured sequentially, and the LUC/REN ratio was calculated as the final transcriptional activity. B. ChIP assay results. FHCs with either knockdown or overexpression of FOXO3 were subjected to ChIP with rabbit anti-FOXO3. Precipitated DNA was subjected to qPCR analysis with primers probed to the PPM1B promoter. Asterisks indicate significant differences (***P<0.001). Independent experiments were repeated performed to calculate mean values.

FOXO3 directly regulated PPM1B transcription in FHCs

The above results indicated that PPM1B plays a key role in the cytotoxic and pro-inflammatory effects of TcdB in FHCs. We explored the promoter sequence of PPM1B with commercial tools (http://www.genecopoeia.com/product/search/index.php?prt=1) and then predicted the possible transcription factor targeted to this sequence using an online protocol (http://alggen.lsi.upc.es/cgi-bin/promo_v3/promo/promoinit.cgi?dirDB=TF_8.3). One major common transcription factor with the highest score, FOXO3 (also known as FOXO3a), was selected as the candidate (data not shown) for the following experiments.

We implemented a dual-luciferase reporter assay to test this prediction. The PPM1B promoter-driven LUC (pGL3-basic-PPM1B-p) and pRL Renilla luciferase control reporter vector were cotransfected into FHCs. Forty-eight hours later, the activities of firefly luciferase (LUC) and Renilla luciferase (REN) were measured sequentially. We monitored the ratio of LUC/REN, which reflects FOXO3 transcriptional activity. As shown in **Figure 4A**, compared with the vector control that was transfected with the empty construct (LUC/REN: 38.2±0.9), FOXO3 overexpression significantly increased the ratio (LUC/REN: 78.5±2.1, P<0.001), while the knockdown of FOXO3 significantly decreased the ratio (LUC/REN: 13.9±0.2, P< 0.001), suggesting that FOXO3 activated the transcription of PPM1B.

To further validate the binding of FOXO3 to the promoter of the PPM1B gene, we performed chromatin immunoprecipitation (ChIP) in FHCs with FOXO3 overexpression and knockdown. Compared to the vector control cells, PPM1B was highly enriched in FOXO3-overexpressing cells, while the signals for the promoter of PPM1B decreased significantly upon knockdown of FOXO3 (**Figure 4B**). These results demonstrated that FOXO3 binds to the promoter sequence and directly regulates PPM1B transcription. On this basis, we can conclude that FOXO3/PPM1B participated in the inflammatory reactions caused by TcdB in FHC by upregulating NF-κB transcriptional activity.

TcdB treatment induced increased phosphorylation in the AKT/FOXO3 pathway in FHCs

According to previous reports, the potency of FOXO3 is elaborately regulated by phosphorylation [29]. AKT can directly phosphorylate FOXO3 at the S253 residue, which determines the nuclear/cytoplasmic shuttling of FOXO3 [29]. Specifically, FOXO3 phosphorylated by AKT is mainly localized to the cytoplasm, which prevents its transcriptional activity [29, 30]. Thus, we assessed the effects of TcdB on the expression and inactivation of FOXO3 3 h after administration. As shown in **Figure 5A**, **5B** and Supplementary Figure 5, treatment significantly increased the phosphorylation of FOXO3 at S253 at both concentrations (P<0.001). In comparison, TcdB did not change the total amount of FOXO3 protein, suggesting that TcdB decreased the protein's transcriptional activity.

Given the key role of AKT in regulating FOXO3 transcriptional potency, we also evaluated AKT activation in TcdB-treated FHCs. As shown in **Figure 5A** and **5B**, treatment enhanced AKT phosphorylation at T308 (P<0.05 at 1000 ng/

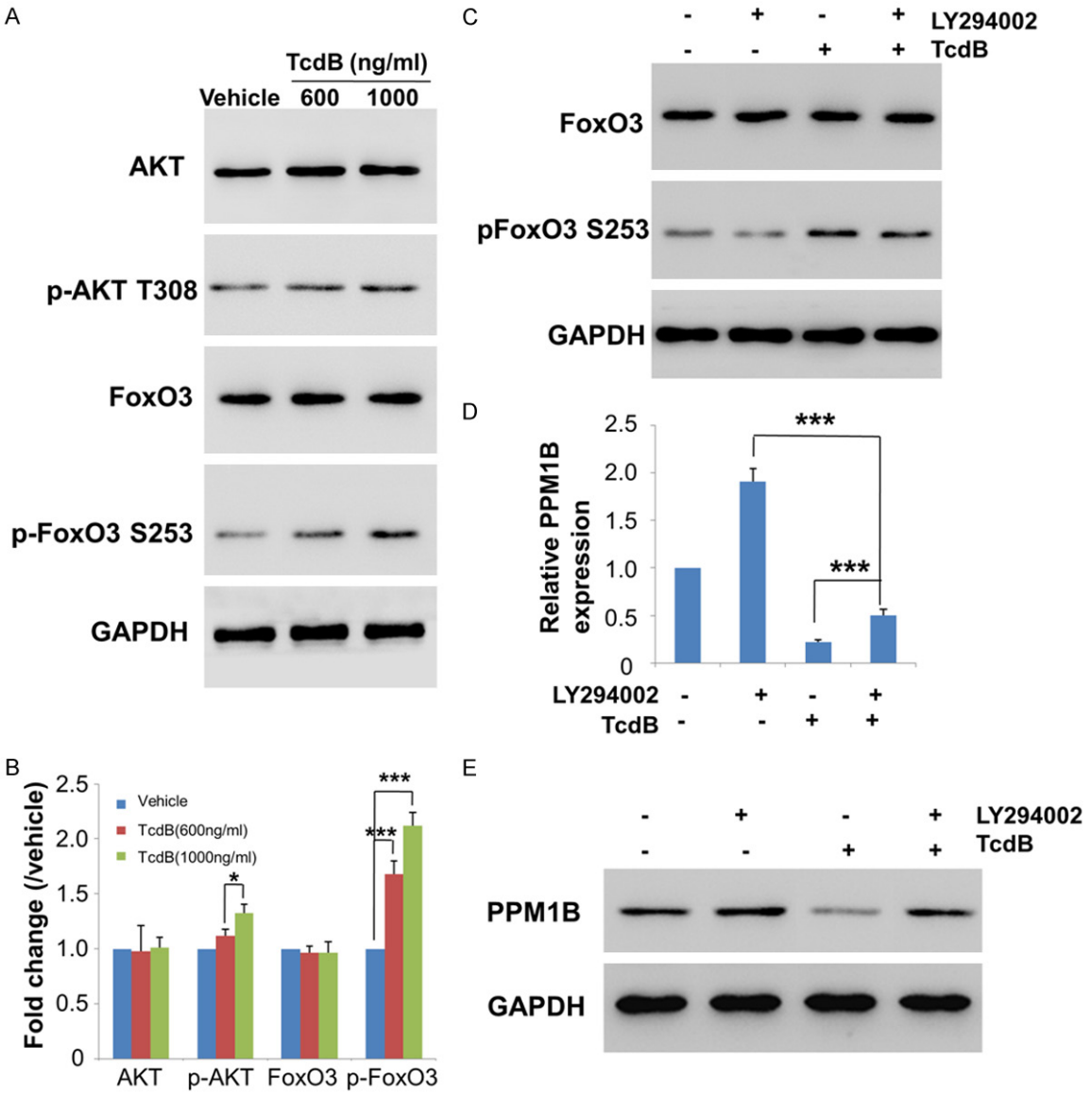

Figure 5. TcdB treatment increased phosphorylation of AKT/FOXO3 to enhance signaling in FHCs. (A, B) FHCs were treated with TcdB (600 or 1,000 ng/mL) for 3 h. AKT and FOXO3 expression and phosphorylation in FHCs were evaluated by western blot analysis. Representative blots (A) and quantitative results (B) are shown. (C-E) TcdB-treated FHCs were exposed to the phosphoinositide 3-kinase inhibitor LY294002. The expression and phosphorylation of FoxO3 (C), transcription of PPM1B at the mRNA level (D), and expression of PPM1B at the protein level (E) were assessed. Asterisks indicate significant differences ($^{*}P<0.05$, $^{***}P<0.001$). Independent experiments were repeated performed to calculate mean values.

ml) but had no effect on the total amount of protein. Collectively, these results indicated that TcdB induced inflammation in FHCs, possibly through activating the AKT/FOXO3 signaling pathway, which downregulates PPM1B transcription.

AKT inhibition increased PPM1B expression in TcdB-treated FHCs

To confirm the direct regulation of PPM1B expression by AKT, we exposed TcdB-treated FHCs to the chemical inhibitor LY294002 (5 μM), which can inactivate AKT [43]. Then, we assessed the expression and phosphorylation of FOXO3 and PPM1B after 3 h and 24 h. Our results showed that AKT inhibition significantly reduced FOXO3 phosphorylation at S253 in TcdB-treated cells (**Figure 5C** and Supplementary Figure 6), which is consistent with the above findings. Moreover, AKT inhibition also led to increased expression of PPM1B at mRNA (**Figure 5D**) and protein levels (**Figure 5E**

and Supplementary Figure 7), suggesting a direct relationship between AKT activity and PPM1B expression. Taken together, these data indicate that PPM1B is directly regulated by the AKT/FOXO3 signaling pathway in FHCs, which may at least partially account for the molecular mechanism of TcdB-induced colonic inflammation.

In vivo study of inflammation-induced effects of TcdB and therapeutic potential of AKT inhibition

The above results suggest that TcdB induced an inflammatory response in human colon epithelial cells at least partially due to activation of AKT/FOXO3 signaling, which can further downregulate the transcription of PPM1B, enhance the transcriptional activity of NF-κB, and eventually stimulate the production of endogenous pro-inflammatory cytokines. To study the role of the AKT/FOXO3/PPM1B pathway in the context of TcdB-induced colonic inflammation, we constructed a mouse model of *C. difficile* infection. The mice were euthanized 1 and 3 days after infection, and changes in colonic tissues and serum levels of IL-6 and TNF-α were measured. H&E staining of colonic tissues is shown in **Figure 6**. The structure of the colonic mucosa was normal in the normal control group at 1d/3d, with no mucosal congestion or edema and no inflammatory cell infiltration. In contrast, an irregularly arranged structure was observed in the model group both time points, and the lamina propria was markedly hyperemic and edematous. Substantial inflammatory cell infiltration was observed in the mucosa and submucosa. In the LY294002 treatment group, the colonic mucosa structure was still intact, the mucosal layer and submucosal lamina propria were congested, edema was mild, and inflammatory cell infiltration was reduced. For clarity, we also calculated histological scores according to a previous report (**Table 2**) [44]. Compared with the blank control, *C. difficile* infection exacerbated intestinal injury, whereas treatment with the PI3K/AKT signaling inhibitor LY294002 (5 mg/kg for 1 or 3 days before surgery) largely alleviated these changes. Compared to the blank control, which showed a normal cellular configuration without edema and inflammatory cell infiltration (**Figure 6A** and **6D**), *C. difficile* infection resulted in damaged colon mucosa tissue with clear submucosal edema and swelling and the presence of neutrophils (**Figure 6B** and **6E**). In contrast, LY294002 (5 mg/kg) decreased the number of invading inflammatory cells and alleviated submucosal edema and swelling (**Figure 6C** and **6F**).

We examined the production of pro-inflammatory cytokines in peripheral blood samples using ELISAs. Similar results were observed among the different treatments, which lasted for 1 day and 3 days (**Figure 6G**). Infection with *C. difficile* significantly increased serum IL-6, which was largely reduced by treatment with LY294002. We also measured the concentrations of IL-6 and TNF-α at colonic tissue levels (**Figure 6I**), which were consistent with the findings in serum (**Figure 6G**). Furthermore, we determined the expression and phosphorylation of selected molecules by western blotting analysis. There was no significant difference between treatments at different time points (1 day or 3 days). Infection with *C. difficile* enhanced the phosphorylation of AKT and NF-kB p65 at T308 and S536, respectively, without changing the total amounts of the proteins and decreased the expression of PPM1B (**Figure 6H** and Supplementary Figure 8). Compared with the model group, LY294002 significantly reversed these effects by downregulating phosphorylated AKT and NF-kB p65 and increasing PPM1B expression (**Figure 6H** and Supplementary Figure 8). Collectively, our *in vivo* studies confirmed that *C. difficile* induced colonic damage through the AKT/FOXO3/PPM1B pathway.

We also assessed cytokine levels in TcdB-treated FHCs in the presence of the AKT pathway inhibitor. Compared with our previous results (**Figure 1D**, **1E**), AKT inhibition by LY294002 largely prevented the TcdB-induced increases in the expression and secretion of both IL-6 and TNF-α (**Figure 7A**, **7B**).

Discussion

The present study confirmed that TcdB can induce significant cell growth inhibition and apoptosis in FHCs. It is worth noting that FHCs are relatively resistant to apoptosis induction according to a previous report [45]. Our results imply strong cytotoxicity of TcdB, which agrees with the contribution of TcdB to virulence. We also observed elevated IL-6 and TNF-α levels

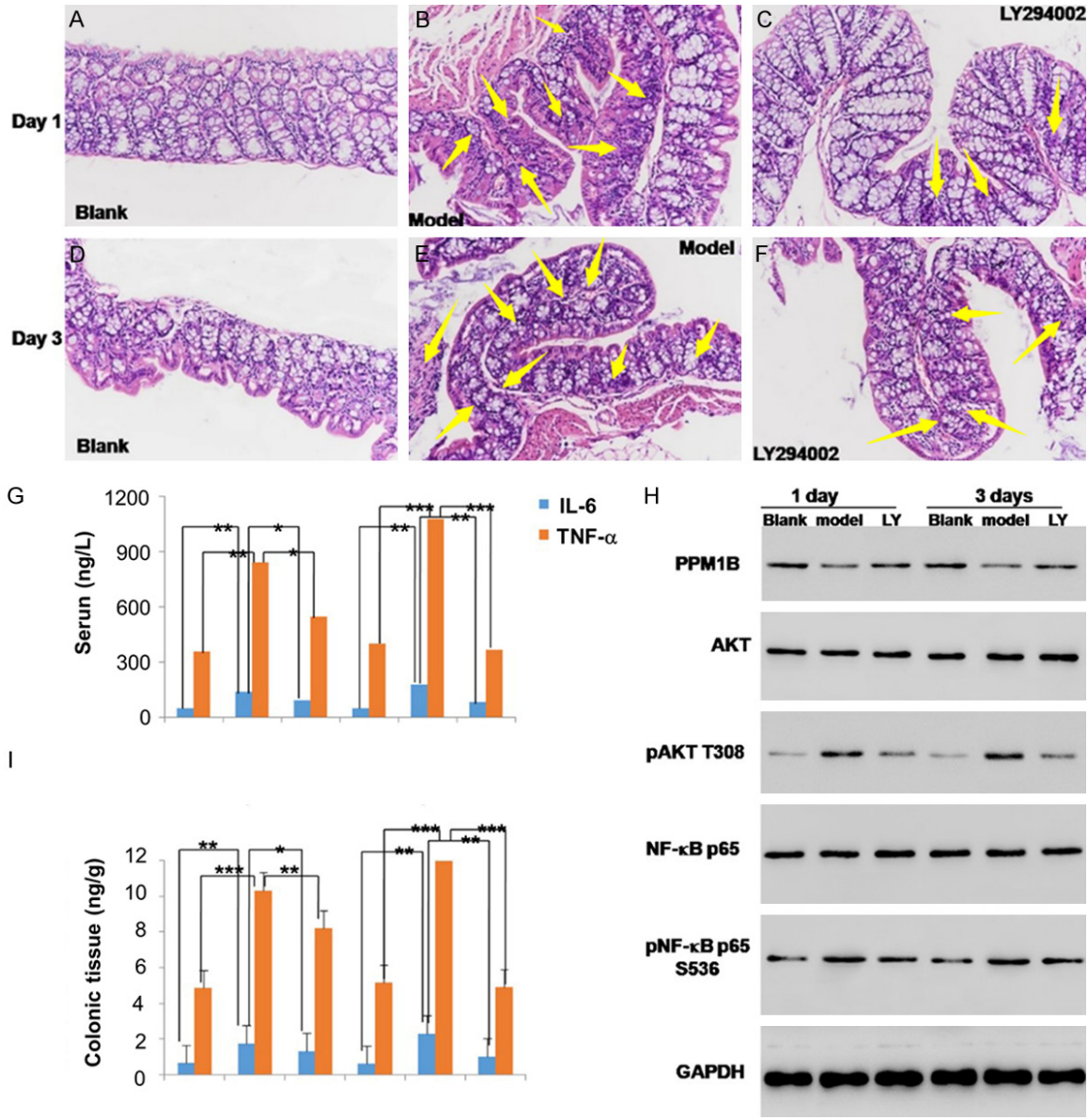

Figure 6. *In vivo* studies of the effects of LY294002 treatment in the *C. difficile*-infected mouse model. Mice were randomly divided into three groups (n=12). Mice in the blank group received a single intragastric administration of saline (0.5 mL) on day 0 as a control. Mice in the model group were intragastrically administered *C. difficile* (1×108 CFU/mouse) on day 0. After intragastric administration of *C. difficile* (1×108 CFU/mouse) on day 0, mice in the drug treatment group received a daily intraperitoneal injection of LY294002 (5 mg/kg) until the mice were euthanized (s6 mice/group on days 1 and 3). A-F. Representative H&E staining results for mouse colon tissues. A and D. Colonic tissues from representative mice in the blank control group showed normal cell configuration without edema or inflammatory cell infiltration. B and E. Colon mucosa tissues from representative mice in the model group showed marked submucosal edema and swelling and the presence of neutrophils. C and F. Treatment with LY294002 (5 mg/kg) decreased the number of invading inflammatory cells and alleviated submucosal edema and swelling. G and I. Production of the pro-inflammatory cytokines IL-6 and TNF-α in serum and colonic tissue. H. Expression and phosphorylation of AKT, NF-κB p65, and PPM1B. Asterisks indicate significant differences (***P<0.001). Independent experiments were repeated performed to calculate mean values.

following TcdB administration. These pro-inflammatory cytokines have been implicated as important mediators of the inflammatory reaction in patients with intestinal inflammation. Xiao et al. recently found that neutralization of IL-6 and TNF-α ameliorated intestinal permea-

Table 2. Histological assessments by treatment group

Index	Grouping	Sample number	Picture number	Amplification	Intestinal epithelial inflammation score[a]	Inflammatory area score[b]	Histological score[c]
HE	Control 1d	D1	1	×200	0	0	0
		D2	2	×200	0	0	0
		D3	3	×200	0	0	0
	Model 1d	M4	4	×200	2	1	2
		M5	5	×200	3	1	3
		M6	6	×200	1	1	1
	LY294002 1d	L7	7	×200	1	1	1
		L8	8	×200	1	1	1
		L9	9	×200	2	1	2
	Control 3d	D10	10	×200	0	0	0
		D11	11	×200	0	0	0
		D12	12	×200	1	1	1
	Model 3d	M13	13	×200	3	1	3
		M14	14	×200	3	2	6
		M15	15	×200	3	2	6
	LY294002 3d	L16	16	×200	1	2	2
		L17	17	×200	2	1	2
		L18	18	×200	3	1	3

[a]Intestinal epithelial inflammation score: normal mucosa, 0 points; destruction of 1/3 of the bottom of the crypt, 1 point; destruction of 2/3 of the bottom of the crypt, 2 points; destruction of 2/3 of the bottom of the crypt but the epithelium was present, 3 points; destruction of the entire crypt, 4 points. [b]Inflammatory area score: 1-25%, 1 point; 26-50%, 2 points; 51-75%, 3 points; 76-100%, 4 points. [c]The histological score is the product of the intestinal epithelial inflammation score and the inflammation area score.

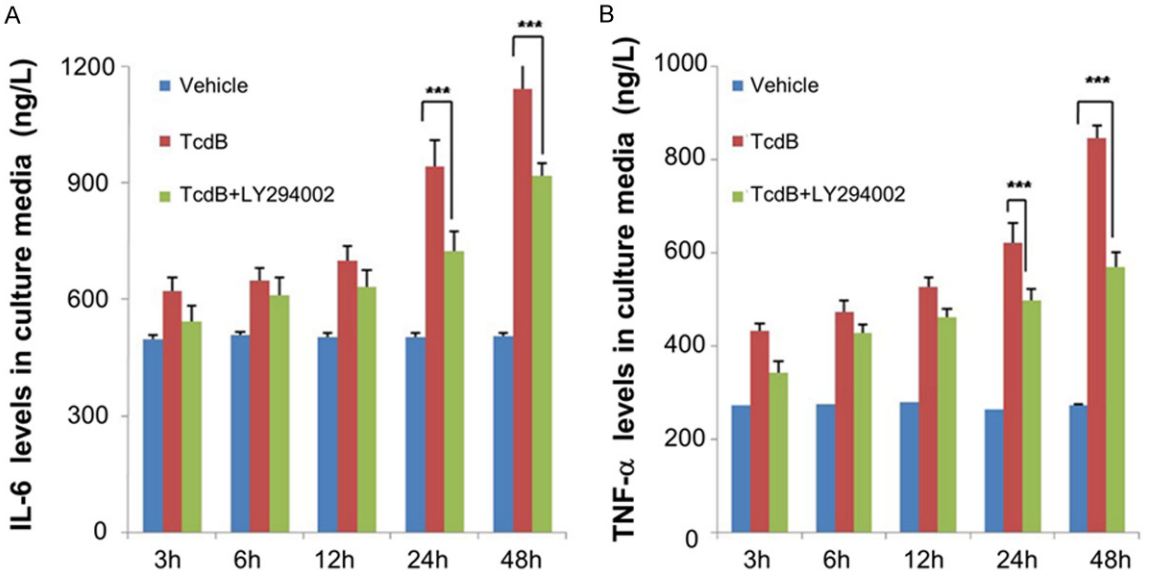

Figure 7. Inhibition of AKT signaling significantly reduced the expression and secretion of IL-6 and TNF-α in FHCs. TcdB-treated FHCs were exposed to the phosphoinositide 3-kinase inhibitor LY294002. Changes in IL-6 (A) and TNF-α (B) release were determined by ELISA. Asterisks indicate significant differences (***P<0.001) between LY294002+TcdB- and TcdB-treated cells. Independent experiments were repeated performed to calculate mean values.

bility in induced colitis [46], suggesting key roles for these proteins in the pathogenesis and therapies of intestinal inflammation. Taken together, these findings demonstrate the molecular basis in the context of TcdB-induced intestinal injury.

The mechanism underlying TcdB-induced intestinal inflammation (*e.g.,* colitis) remains largely unknown. We explored the potential signaling pathway regulating the production of pro-inflammatory cytokines. First, we focused on the upstream regulator NF-κB p65, which plays an essential role in the transcription and expression of IL-6 and TNF-α. We observed significantly elevated phosphorylation of NF-κB p65 at S536 following TcdB administration, which indicated canonical NF-κB transcriptional activation and accounts for the enhanced release of IL-6 and TNF-α. Notably, these findings are consistent with the previous reports [47]. To further understand this process, we attempted to gain insight into the mechanism underlying the increased phosphorylation and activity of NF-κB p65. Previous studies indicated that the phosphorylation level of NF-κB p65 is regulated by numerous protein kinases and some phosphatases [24, 25]. We assessed the expression of selected phosphatases closely related to NF-κB p65. We found that downregulation of PPM1B was the most significant effect induced by TcdB, and its overexpression effectively blocked the cytotoxic and inflammation-induced effects of TcdB. Together, these results prompted us to hypothesize that PPM1B may mediate TcdB-induced inflammation in FHCs. It is worth mentioning that we cannot exclude the effects of other kinases, which were reported to be responsible for the phosphorylation of NF-κB p65, including protein kinase A [48], IkB kinase [49], AKT [50], extracellular signal-regulated kinase [50], and others [51]. This aspect of the signaling pathway constitutes our parallel independent follow-up studies, which could be published in the near future.

With confidence regarding the contribution of PPM1B, we further predicted which upstream transcription factor regulates its expression. Consequently, FOXO3 was recognized as a direct binder to the promoter sequence and a regulator of PPM1B transcription, which was confirmed by both dual-luciferase reporter and ChIP assays. Moreover, TcdB treatment increased the phosphorylation of FOXO3 at S253 and AKT at T308, sites that are responsible for preventing the transcriptional activity of FOXO3 by promoting its relocation to the cytoplasm. Collectively, we can conclude that TcdB induced inflammation in FHCs possibly through activating the AKT/FOXO3 signaling pathway, which downregulated PPM1B transcription and limited pro-inflammatory cytokine release. Our *in vivo* studies confirmed the potential role of the AKT/FOXO3/PPM1B cascade in the context of colonic inflammation caused by TcdB.

Although TcdB was already established as an inflammatory enterotoxin, the molecular mechanisms underlying its activation of innate immunity and stimulation of pro-inflammatory cytokine release are still unclear [7]. To our knowledge, this study is the first report revealing the contribution of the AKT/FOXO3/PPM1B pathway to the pathogenesis of TcdB-induced colonic inflammation. We also showed that AKT inhibition (*e.g.,* LY294002 treatment) could be helpful for diseases such as colitis. These findings, especially the identification of the essential signaling proteins, will help guide targeted drug development against TcdB-induced colitis in the future. Interestingly, the change in the phosphorylation of AKT T308 following *C. difficile* infection seemed more significant *in vivo* than in FHCs (**Figures 5A** and **6H**), which could be attributable to alternative pathways or more complicated mechanisms that remain unknown and will be explored in future work.

In conclusion, we systematically investigated the effects of TcdB on FHCs and the potential mechanism underlying TcdB-induced colitis. Recombinant TcdB protein had strong antiproliferative effects and induced considerable apoptosis in FHCs. TcdB also stimulated inflammatory cytokine production and NF-κB p65 phosphorylation. Regarding the molecular mechanism, we demonstrated that PPM1B plays a central role in mediating the TcdB-induced inflammatory response. Further studies indicated that AKT/FOXO3 signaling could at least partially account for the downregulation of PPM1B expression in TcdB-treated cells. Moreover, *in vivo* studies in a mouse model infected with *C. difficile* and treated with an inhibitor confirmed the molecular mechanism and implied promise for future treatment.

Collectively, we concluded that TcdB induced colonic inflammation by regulating the AKT/FOXO3/PPM1B pathway.

Acknowledgements

This work was supported by grants from National Natural Science Foundation of China (81471537 and 81603163), the Interdisciplinary Project of "Clinical Immunology of Traditional Chinese Medicine" in Shanghai (No. 30304113598), and the Natural Science Foundation of Shanghai (18ZR1405500).

Disclosure of conflict of interest

None.

Address correspondence to: Yijian Chen, Institute of Antibiotics, Huashan Hospital, Fudan University, Building 6, 12 M., Wulumuqi Road, Shanghai 200040, China. Tel: +86-21-52888195; E-mail: chenyijiansh@hotmail.com; Yuejuan Zheng, Department of Immunology and Microbiology, Shanghai University of Traditional Chinese Medicine; 46#, 1200 Cailun Road, Shanghai 201203, China. Tel: +86-21-51322150; E-mail: zhengyj@shutcm.edu.cn

References

[1] Elliott B, Chang BJ, Golledge CL and Riley TV. Clostridium difficile-associated diarrhoea. Intern Med J 2007; 37: 561-568.

[2] Poutanen SM and Simor AE. Clostridium difficile-associated diarrhea in adults. CMAJ 2004; 171: 51-58.

[3] Loo VG, Poirier L, Miller MA, Oughton M, Libman MD, Michaud S, Bourgault AM, Nguyen T, Frenette C, Kelly M, Vibien A, Brassard P, Fenn S, Dewar K, Hudson TJ, Horn R, Rene P, Monczak Y and Dascal A. A predominantly clonal multi-institutional outbreak of Clostridium difficile-associated diarrhea with high morbidity and mortality. N Engl J Med 2005; 353: 2442-2449.

[4] McDonald LC, Killgore GE, Thompson A, Owens RC Jr, Kazakova SV, Sambol SP, Johnson S and Gerding DN. An epidemic, toxin gene-variant strain of Clostridium difficile. N Engl J Med 2005; 353: 2433-2441.

[5] Kelly CP and Kyne L. The host immune response to Clostridium difficile. J Med Microbiol 2011; 60: 1070-1079.

[6] Madan R, Guo X, Naylor C, Buonomo EL, Mackay D, Noor Z, Concannon P, Scully KW, Pramoonjago P, Kolling GL, Warren CA, Duggal P and Petri WA Jr. Role of leptin-mediated colonic inflammation in defense against Clostridium difficile colitis. Infect Immun 2014; 82: 341-349.

[7] Shen A. Clostridium difficile toxins: mediators of inflammation. J Innate Immun 2012; 4: 149-158.

[8] Burdon DW, George RH, Mogg GA, Arabi Y, Thompson H, Johnson M, Alexander-Williams J and Keighley MR. Faecal toxin and severity of antibiotic-associated pseudomembranous colitis. J Clin Pathol 1981; 34: 548-551.

[9] Lyerly DM, Saum KE, MacDonald DK and Wilkins TD. Effects of Clostridium difficile toxins given intragastrically to animals. Infect Immun 1985; 47: 349-352.

[10] Lyras D, O'Connor JR, Howarth PM, Sambol SP, Carter GP, Phumoonna T, Poon R, Adams V, Vedantam G, Johnson S, Gerding DN and Rood JI. Toxin B is essential for virulence of Clostridium difficile. Nature 2009; 458: 1176-1179.

[11] Kuehne SA, Cartman ST, Heap JT, Kelly ML, Cockayne A and Minton NP. The role of toxin A and toxin B in Clostridium difficile infection. Nature 2010; 467: 711-713.

[12] Bezerra Lima B, Faria Fonseca B, da Graca Amado N, Moreira Lima D, Albuquerque Ribeiro R, Garcia Abreu J and de Castro Brito GA. Clostridium difficile toxin A attenuates Wnt/beta-catenin signaling in intestinal epithelial cells. Infect Immun 2014; 82: 2680-2687.

[13] Carbonell P, Fichera D, Pandit SB and Faulon JL. Enumerating metabolic pathways for the production of heterologous target chemicals in chassis organisms. BMC Syst Biol 2012; 6: 10.

[14] Lica M, Schulz F, Schelle I, May M, Just I and Genth H. Difference in the biological effects of Clostridium difficile toxin B in proliferating and non-proliferating cells. Naunyn Schmiedebergs Arch Pharmacol 2011; 383: 275-283.

[15] Welsh CF, Roovers K, Villanueva J, Liu Y, Schwartz MA and Assoian RK. Timing of cyclin D1 expression within G1 phase is controlled by Rho. Nat Cell Biol 2001; 3: 950-957.

[16] Chen S, Sun C, Wang H and Wang J. The role of Rho GTPases in toxicity of Clostridium difficile toxins. Toxins (Basel) 2015; 7: 5254-5267.

[17] Sehr P, Joseph G, Genth H, Just I, Pick E and Aktories K. Glucosylation and ADP ribosylation of rho proteins: effects on nucleotide binding, GTPase activity, and effector coupling. Biochemistry 1998; 37: 5296-5304.

[18] Qa'Dan M, Ramsey M, Daniel J, Spyres LM, Safiejko-Mroczka B, Ortiz-Leduc W and Ballard JD. Clostridium difficile toxin B activates dual caspase-dependent and caspase-independent apoptosis in intoxicated cells. Cell Microbiol 2002; 4: 425-434.

[19] Xu H, Yang J, Gao W, Li L, Li P, Zhang L, Gong YN, Peng X, Xi JJ, Chen S, Wang F and Shao F. Innate immune sensing of bacterial modifications of Rho GTPases by the Pyrin inflammasome. Nature 2014; 513: 237-241.

[20] Cowardin CA, Kuehne SA, Buonomo EL, Marie CS, Minton NP and Petri WA Jr. Inflammasome activation contributes to interleukin-23 production in response to Clostridium difficile. MBio 2015; 6: e02386-14.
[21] Farrow MA, Chumbler NM, Lapierre LA, Franklin JL, Rutherford SA, Goldenring JR and Lacy DB. Clostridium difficile toxin B-induced necrosis is mediated by the host epithelial cell NADPH oxidase complex. Proc Natl Acad Sci U S A 2013; 110: 18674-18679.
[22] Di Bella S, Ascenzi P, Siarakas S, Petrosillo N and di Masi A. Clostridium difficile Toxins A and B: insights into pathogenic properties and extraintestinal effects. Toxins (Basel) 2016; 8: 134.
[23] Yasumoto K, Okamoto S, Mukaida N, Murakami S, Mai M and Matsushima K. Tumor necrosis factor alpha and interferon gamma synergistically induce interleukin 8 production in a human gastric cancer cell line through acting concurrently on AP-1 and NF-kB-like binding sites of the interleukin 8 gene. J Biol Chem 1992; 267: 22506-22511.
[24] Chew J, Biswas S, Shreeram S, Humaidi M, Wong ET, Dhillion MK, Teo H, Hazra A, Fang CC, Lopez-Collazo E, Bulavin DV and Tergaonkar V. WIP1 phosphatase is a negative regulator of NF-kappaB signalling. Nat Cell Biol 2009; 11: 659-666.
[25] Li S, Wang L, Berman MA, Zhang Y and Dorf ME. RNAi screen in mouse astrocytes identifies phosphatases that regulate NF-kappaB signaling. Mol Cell 2006; 24: 497-509.
[26] Sun W, Yu Y, Dotti G, Shen T, Tan X, Savoldo B, Pass AK, Chu M, Zhang D, Lu X, Fu S, Lin X and Yang J. PPM1A and PPM1B act as IKKbeta phosphatases to terminate TNFalpha-induced IKKbeta-NF-kappaB activation. Cell Signal 2009; 21: 95-102.
[27] Zhao Q, Wang X, Nelin LD, Yao Y, Matta R, Manson ME, Baliga RS, Meng X, Smith CV, Bauer JA, Chang CH and Liu Y. MAP kinase phosphatase 1 controls innate immune responses and suppresses endotoxic shock. J Exp Med 2006; 203: 131-140.
[28] Gil-Araujo B, Toledo Lobo MV, Gutierrez-Salmeron M, Gutierrez-Pitalua J, Ropero S, Angulo JC, Chiloeches A and Lasa M. Dual specificity phosphatase 1 expression inversely correlates with NF-kappaB activity and expression in prostate cancer and promotes apoptosis through a p38 MAPK dependent mechanism. Mol Oncol 2014; 8: 27-38.
[29] Nho RS and Hergert P. FoxO3a and disease progression. World J Biol Chem 2014; 5: 346-354.
[30] Santo EE, Stroeken P, Sluis PV, Koster J, Versteeg R and Westerhout EM. FOXO3a is a major target of inactivation by PI3K/AKT signaling in aggressive neuroblastoma. Cancer Res 2013; 73: 2189-2198.
[31] Zufferey R, Nagy D, Mandel RJ, Naldini L and Trono D. Multiply attenuated lentiviral vector achieves efficient gene delivery in vivo. Nat Biotechnol 1997; 15: 871-875.
[32] Weinmann AS, Bartley SM, Zhang T, Zhang MQ and Farnham PJ. Use of chromatin immunoprecipitation to clone novel E2F target promoters. Mol Cell Biol 2001; 21: 6820-6832.
[33] Lv Z, Peng G, Liu W, Xu H and Su J. Berberine blocks the relapse of Clostridium difficile infection in C57BL/6 mice after standard vancomycin treatment. Antimicrob Agents Chemother 2015; 59: 3726-3735.
[34] Johal SS, Solomon K, Dodson S, Borriello SP and Mahida YR. Differential effects of varying concentrations of clostridium difficile toxin A on epithelial barrier function and expression of cytokines. J Infect Dis 2004; 189: 2110-2119.
[35] Kasendra M, Barrile R, Leuzzi R and Soriani M. Clostridium difficile toxins facilitate bacterial colonization by modulating the fence and gate function of colonic epithelium. J Infect Dis 2014; 209: 1095-1104.
[36] Huang T, Li S, Li G, Tian Y, Wang H, Shi L, Perez-Cordon G, Mao L, Wang X, Wang J and Feng H. Utility of Clostridium difficile toxin B for inducing anti-tumor immunity. PLoS One 2014; 9: e110826.
[37] Tam J, Beilhartz GL, Auger A, Gupta P, Therien AG and Melnyk RA. Small molecule inhibitors of Clostridium difficile toxin B-induced cellular damage. Chem Biol 2015; 22: 175-185.
[38] LaFrance ME, Farrow MA, Chandrasekaran R, Sheng J, Rubin DH and Lacy DB. Identification of an epithelial cell receptor responsible for Clostridium difficile TcdB-induced cytotoxicity. Proc Natl Acad Sci U S A 2015; 112: 7073-7078.
[39] Li Q and Verma IM. NF-kappaB regulation in the immune system. Nat Rev Immunol 2002; 2: 725-734.
[40] Sen R and Baltimore D. Inducibility of kappa immunoglobulin enhancer-binding protein Nf-kappa B by a posttranslational mechanism. Cell 1986; 47: 921-928.
[41] Tak PP and Firestein GS. NF-kappaB: a key role in inflammatory diseases. J Clin Invest 2001; 107: 7-11.
[42] Huang B, Yang XD, Lamb A and Chen LF. Posttranslational modifications of NF-kappaB: another layer of regulation for NF-kappaB signaling pathway. Cell Signal 2010; 22: 1282-1290.
[43] Semba S, Itoh N, Ito M, Harada M and Yamakawa M. The in vitro and in vivo effects of 2-(4-morpholinyl)-8-phenyl-chromone (LY29400-

2), a specific inhibitor of phosphatidylinositol 3'-kinase, in human colon cancer cells. Clin Cancer Res 2002; 8: 1957-1963.

[44] Dieleman LA, Palmen MJ, Akol H, Bloemena E, Pena AS, Meuwissen SG and Van Rees EP. Chronic experimental colitis induced by dextran sulphate sodium (DSS) is characterized by Th1 and Th2 cytokines. Clin Exp Immunol 1998; 114: 385-391.

[45] Soucek K, Gajduskova P, Brazdova M, Hyzd' alova M, Koci L, Vydra D, Trojanec R, Pernicova Z, Lentvorska L, Hajduch M, Hofmanova J and Kozubik A. Fetal colon cell line FHC exhibits tumorigenic phenotype, complex karyotype, and TP53 gene mutation. Cancer Genet Cytogenet 2010; 197: 107-116.

[46] Xiao YT, Yan WH, Cao Y, Yan JK and Cai W. Neutralization of IL-6 and TNF-alpha ameliorates intestinal permeability in DSS-induced colitis. Cytokine 2016; 83: 189-192.

[47] Batah J, Deneve-Larrazet C, Jolivot PA, Kuehne S, Collignon A, Marvaud JC and Kansau I. Clostridium difficile flagella predominantly activate TLR5-linked NF-kappaB pathway in epithelial cells. Anaerobe 2016; 38: 116-124.

[48] Zhong H, Voll RE and Ghosh S. Phosphorylation of NF-kappa B p65 by PKA stimulates transcriptional activity by promoting a novel bivalent interaction with the coactivator CBP/p300. Mol Cell 1998; 1: 661-671.

[49] Sakurai H, Suzuki S, Kawasaki N, Nakano H, Okazaki T, Chino A, Doi T and Saiki I. Tumor necrosis factor-alpha-induced IKK phosphorylation of NF-kappaB p65 on serine 536 is mediated through the TRAF2, TRAF5, and TAK1 signaling pathway. J Biol Chem 2003; 278: 36916-36923.

[50] Kwon HJ, Choi GE, Ryu S, Kwon SJ, Kim SC, Booth C, Nichols KE and Kim HS. Stepwise phosphorylation of p65 promotes NF-kappaB activation and NK cell responses during target cell recognition. Nat Commun 2016; 7: 11686.

[51] Sasaki CY, Barberi TJ, Ghosh P and Longo DL. Phosphorylation of RelA/p65 on serine 536 defines an I{kappa}B{alpha}-independent NF-{kappa}B pathway. J Biol Chem 2005; 280: 34538-34547.

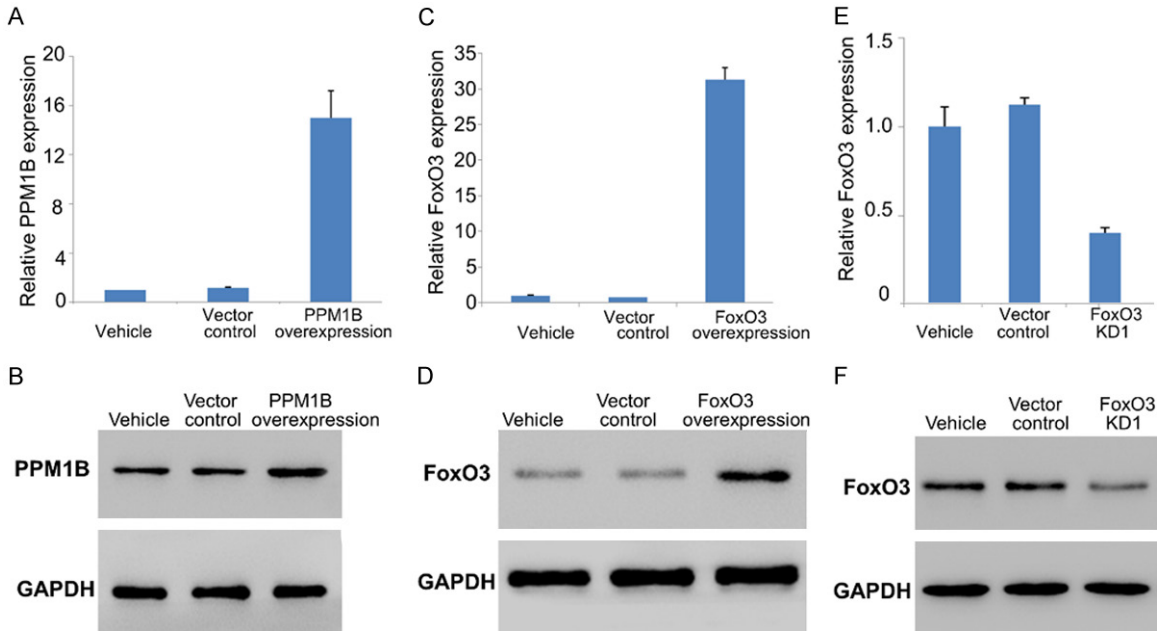

Supplementary Figure 1. FHC cells were infected with PPM1B overexpression, FoxO3 overexpression, FoxO3 knockdown (KD1) or Vector control lentivirus. The alteration of expression of PPM1B and FOXO3 was confirmed by real-time q-PCR (A, C, E) and western blotting (B, D, F).

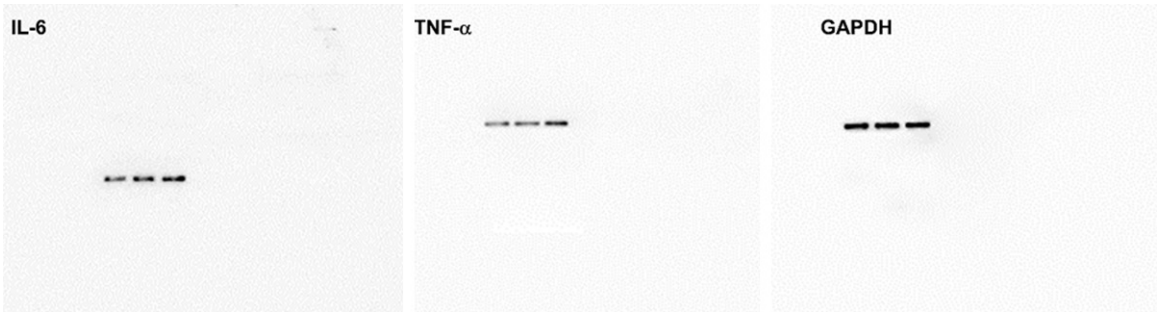

Supplementary Figure 2. Original western images for **Figure 1C**.

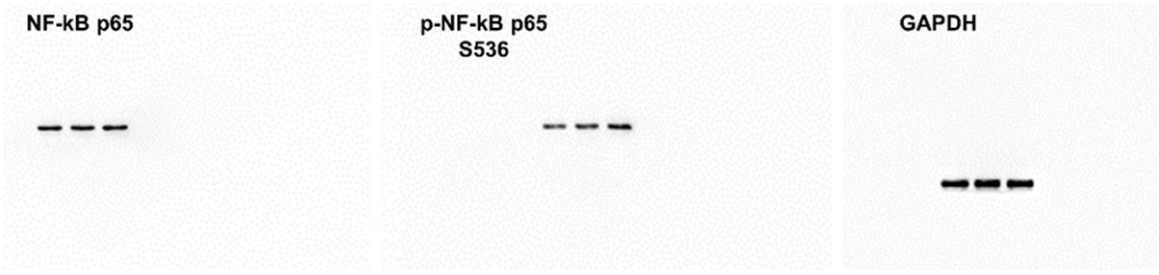

Supplementary Figure 3. Original western images for **Figure 2A**.

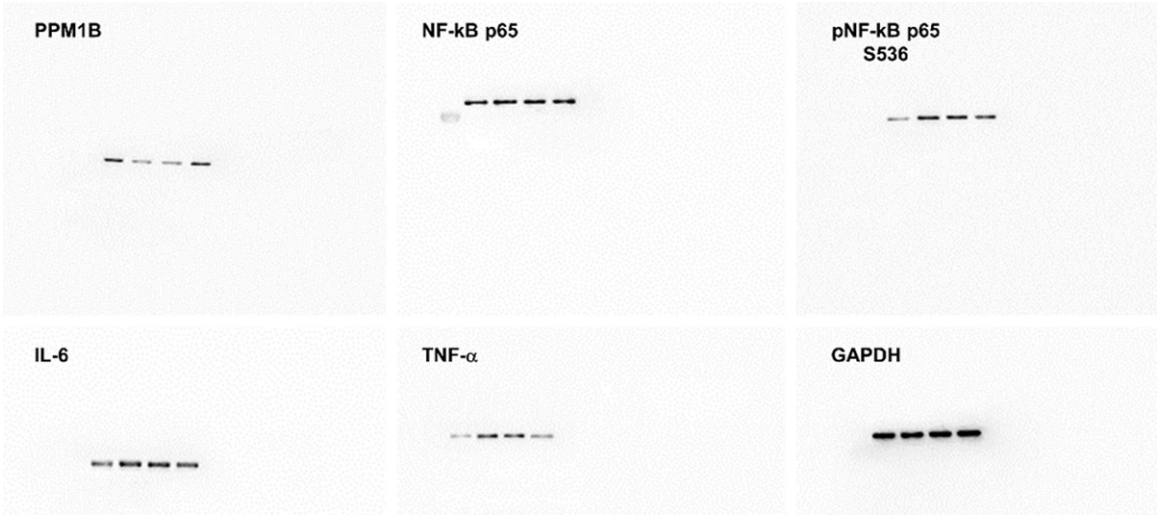

Supplementary Figure 4. Original western images for **Figure 3C**.

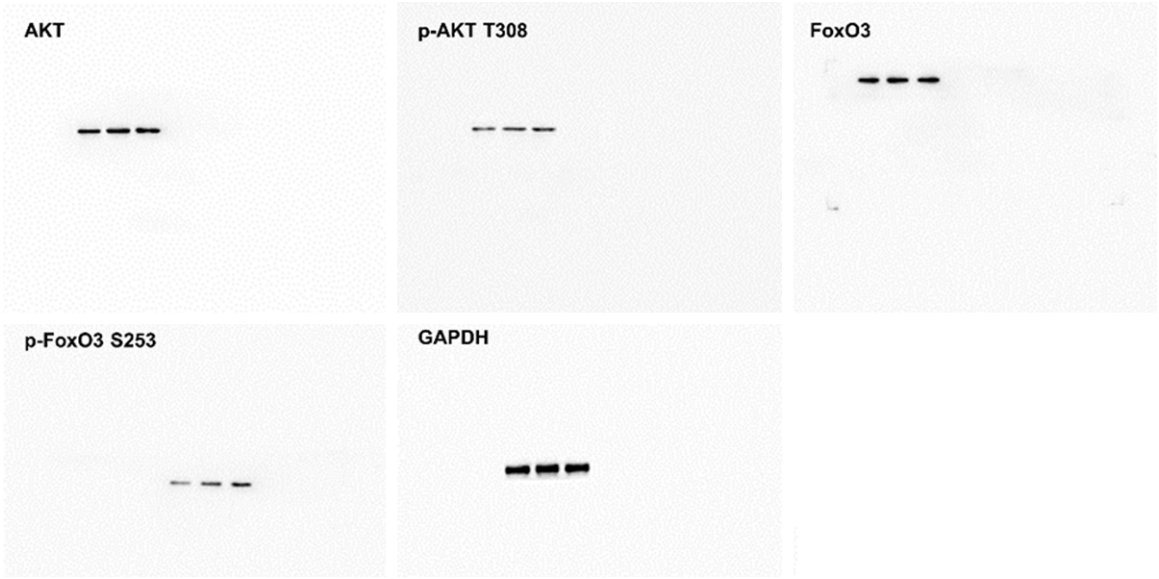

Supplementary Figure 5. Original western images for **Figure 5A**.

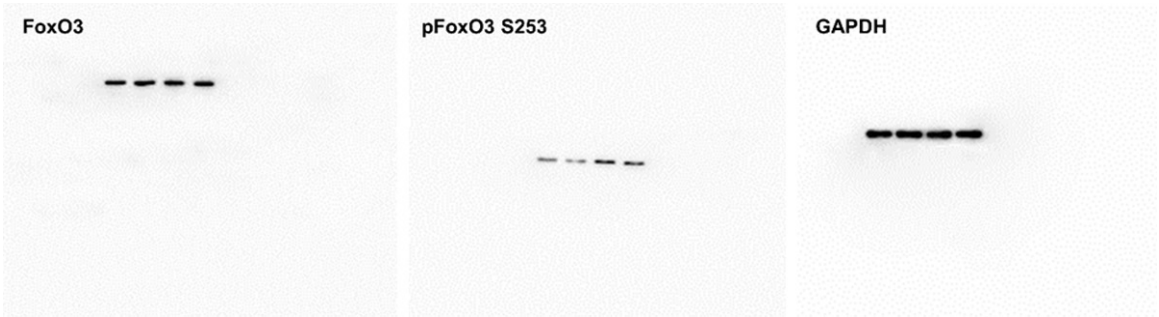

Supplementary Figure 6. Original western images for **Figure 5C**.

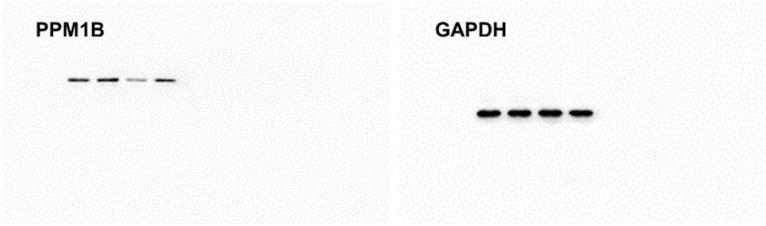

Supplementary Figure 7. Original western images for **Figure 5E**.

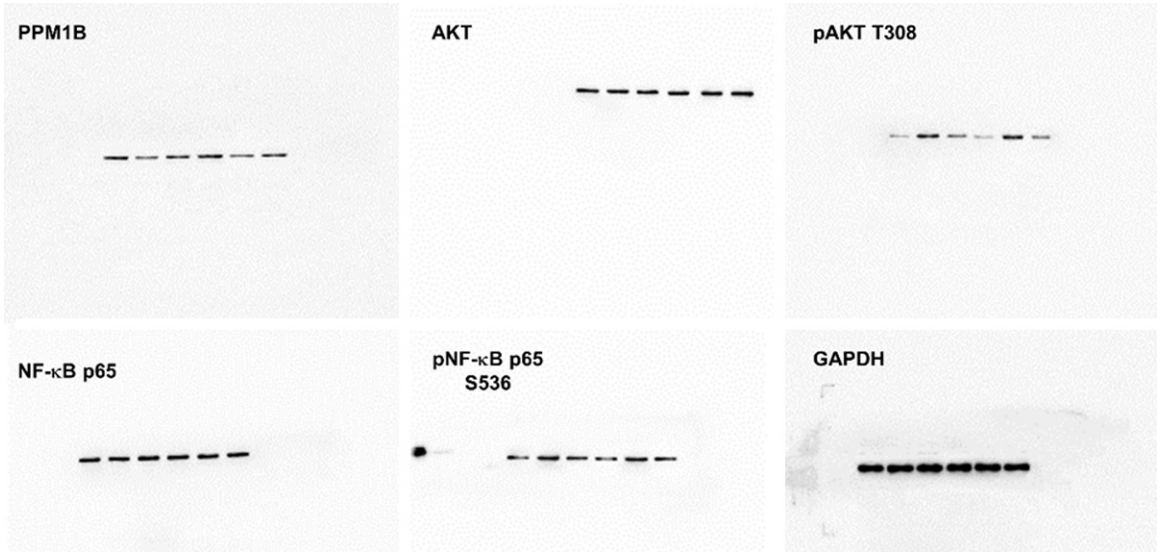

Supplementary Figure 8. Original western images for **Figure 6H**.